

## Fast Catalytic Pyrolysis of Tetradecanoic Acid: Formation of Ketones as Intermediate Compounds in the Production of Hydrocarbons

Mailena Dourado,<sup>1a</sup> Noyala Fonseca,<sup>1a</sup> Roger Fréty<sup>1a,b</sup> and Emerson A. Sales<sup>1\*,a,c</sup>

<sup>a</sup>Laboratório de Bioenergia e Catálise (LABEC), Escola Politécnica, Universidade Federal da Bahia (UFBA), Rua Aristides Novis, 2, 2º andar, Federação, 40210-630 Salvador-BA, Brazil

<sup>b</sup>Departamento de Físico-Química, Instituto de Química, Universidade Federal da Bahia (UFBA), Rua Barão de Jeremoabo, 3º andar, Campus Universitário de Ondina, 40170-290 Salvador-BA, Brazil

<sup>c</sup>Programa de Pós-Graduação em Engenharia Industrial (PEI), Escola Politécnica, Universidade Federal da Bahia (UFBA), Rua Aristides Novis, 2, 6º andar, Federação, 40210-630 Salvador-BA, Brazil

This work aimed to compare two different catalysts in the production of a long chain ketone, intermediate in the production of hydrocarbons, during pyrolysis of tetradecanoic acid as a model fatty acid. The studied variables were the temperature, 450 and 600 °C, and catalysts,  $\gamma$ -Al<sub>2</sub>O<sub>3</sub> and Nb<sub>2</sub>O<sub>5</sub>, the latter has never been studied under such conditions. Pyrolysis experiments were performed in a micro-pyrolyzer coupled to a gas chromatograph with mass spectrometry detector (GC-MS). In all pyrolysis conditions, 14-heptacosanone was formed in varied amounts. Under the best conditions, for pyrolysis at 600 °C, using  $\gamma$ -Al<sub>2</sub>O<sub>3</sub> as catalyst, the yield of 14-heptacosanone was 18% and the yield of hydrocarbons 24%. The major hydrocarbon product obtained was 1-dodecene. Among the partially deoxygenated compounds, the main products were the ketones 14-heptacosanone and 2-pentadecanone. The present experimental work confirmed also the possibility to obtain hydrocarbons having a chain length longer than the chain length of the original fatty acid reagent, due to a ketonization route followed by decarbonylation.

**Keywords:** fast micro-pyrolysis, ketone, tetradecanoic acid, biofuels

### Introduction

Ketonic decarboxylation is one of the routes identified during the deoxygenation of carboxylic acids to obtain hydrocarbons with carbon chain length compatible with liquid fuels.<sup>1,2</sup> The primary reaction between two identical carboxylic acid molecules at temperatures ranging from 400 to 500 °C results in the formation of a symmetrical ketone, carbon dioxide and water, as well as alkenes and alkanes by subsequent reaction.<sup>3</sup> Figure 1 presents a mechanism for conversion of ketones into olefins, as proposed by Billaud *et al.*<sup>4</sup> Vavon and Apchie,<sup>5</sup> two of the pioneers on catalytic ketone formation, have transformed adipic acid at 350 °C to cyclopentanone by passing the acid vapors through a bed of manganese oxide (MnO), obtaining a yield of 80%.

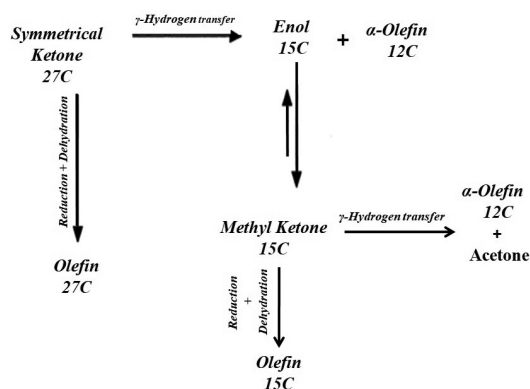


**Figure 1.** Conversion of the symmetrical ketone into alkenes.

The use of catalytic pyrolysis as a route for production of compounds such as ketones and hydrocarbons, from an environmental point of view, can be considered a clean technology, mainly because no solvents or any other elaborated reagents are required. However, many aspects

\*e-mail: eas@ufba.br

Editor handled this article: Jaísa Fernandes Soares

need to be explored, from the choice of the catalyst and the process conditions, to the mechanistic elucidation of the secondary reactions, which depend on the complete identification of the various compounds formed.

The formation of ketone as intermediate has a further advantage: the biofuels produced by this route may have a higher specific energy capacity than that of the reactants, since, in addition to the partial deoxygenation, a kind of condensation of the carbon chains of the carboxylic acids occurs, transforming small molecules into larger ones.<sup>6</sup> Renz<sup>3</sup> reported research results on the yield of long chain ketones as a function of the reaction conditions and the catalysts used, starting from fatty acids and fatty acid esters. Pestman *et al.*<sup>7</sup> studied the ketonization of carboxylic acids in the presence of metal oxides with different M–O bond strengths, and concluded that the higher the bond strength, the greater the conversion to ketones, establishing the sequence:  $\text{PbO}_2 < \text{CuO} < \text{Bi}_2\text{O}_3 < \text{NiO} < \text{MnO}_2 < \text{GeO}_2 < \text{Fe}_2\text{O}_3 < \text{SnO}_2 < \text{V}_2\text{O}_5 < \text{ZnO} < \text{Cr}_2\text{O}_3 < \text{WO}_3 < \text{TiO}_2 < \text{ZrO}_2 < \text{Al}_2\text{O}_3 < \text{MgO}$  and therefore, MgO exhibited the highest production of ketones, when compared to the other oxides in this series. In a more recent paper, Pham *et al.*<sup>8</sup> reviewed the ketonization of carboxylic acids and focused, on one hand, on beta keto-acid and ketene intermediates during the reaction, and on the other hand, on the necessity to use amphoteric catalysts such as cerium oxide to obtain good ketone yields. Kumar *et al.*<sup>9</sup> also detailed the ketonization reaction mechanisms using carboxylic acids and other oxygenated reagents. They stated that the formation of intermediate beta keto-acid is highly probable when using carboxylic acids as feedstock.

Recently, Murzin *et al.*<sup>10</sup> studied the transformation of stearic acid in absence of added catalyst. Using a metallic reactor, a temperature range 300–400 °C, in absence of hydrogen, they observed the formation of 18-pentatriacontanone. Through a kinetic study of their results, the authors showed that depending on stearic acid concentration a zero or first order reaction mechanism could occur. In their conditions, the authors mentioned that the reactor walls can act as catalytic surface to influence the reaction. Also, without catalysts, Qiao *et al.*<sup>11</sup> studied the fast pyrolysis of palm oil between 500 and 650 °C and performed a kinetic analysis. Besides saturated, unsaturated and aromatic hydrocarbons, carbonyl compounds containing ketones, aldehyde, acids, and esters were also detected by gas chromatograph with mass spectrometry (GC-MS). Hasanudin *et al.*<sup>12</sup> studied the hydrocracking of palm oil between 400 and 500 °C, and performed a kinetic analysis, but using a Ni/Mo ZrO<sub>2</sub>-pillared bentonite catalyst, and a fixed bed reactor with longer residence time. Maybe due to this, they did not find carbonyl compounds among the products.

In the presence of hydrogen, however, ketones as intermediates in the conversion of fatty compounds are not observed. For example, during the hydroconversion of saturated triglycerides to hydrocarbons, using alumina supported Ni catalyst, Yenumala *et al.*<sup>13</sup> showed that the first reaction pathway is the transformation of the reactant to saturated fatty acids, followed by the reduction of these fatty acids to aldehydes. Then, both direct decarbonylation of aldehyde to hydrocarbons and/or hydrogenation of aldehyde to fatty alcohol, followed by dehydration to olefin and hydrogenation of the olefin to the corresponding paraffins were observed. The direct decarbonylation was however much more important than the route via alcohol formation. The temperatures used in the production of ketones are generally not higher than 450 °C, whereas space velocities are generally between 1 and 2 h<sup>-1</sup>. It was observed that the thermal processes are slow and lead to different proportions of products, the main being ketones and hydrocarbons.<sup>3</sup>

Recently, Boekaerts and Sels<sup>14</sup> made a deep review on catalytic advancements in carboxylic acid ketonization and its perspectives on biomass valorization. Among many results presented, the authors cited the work of Lee *et al.*,<sup>15</sup> who tested non-model compounds by coupling of fatty acids originating from palm oil hydrolysis (44% palmitic acid, 42% oleic acid, 8% linoleic acid) in a fixed bed pyrolysis reaction at 380 °C using a TiO<sub>2</sub> catalyst. To combat the loss in selectivity and stability, the authors proposed a “hydrogenative hydrolysis” strategy of the palm oil feedstock, which combines the triglyceride hydrolysis and hydrogenation of unsaturated fatty acid species via the presence of a 5% Pt/C catalyst under a 15 bar H<sub>2</sub> reaction atmosphere. Consequently, the fully presaturated fatty acid mixture achieved a higher total ketone yield of 91%, with higher selectivity and time-on-stream stability. Finally, the fatty ketones were subjected to a hydrodeoxygenation step using Pt/Al<sub>2</sub>O<sub>3</sub> at 300 °C under 20 bar H<sub>2</sub>, resulting in ca. 83% C31–C35 alkanes and smaller amounts of C14–C30 hydrocarbon side products with a broader C-number distribution.

The same authors<sup>14</sup> also cited a work of Huo *et al.*,<sup>16</sup> in which after a sequence of bio-derived butyric acid ketonization on ZrO<sub>2</sub>, ketone condensation using Nb<sub>2</sub>O<sub>5</sub> and catalyzed hydrodeoxygenation with Pt/Al<sub>2</sub>O<sub>3</sub>, a hydrocarbon mixture was obtained in 88% C-yield with 56% C-yield of the C14 compound 5-ethyl-4-propylnonane, a drop-in biobased diesel compound.

Fast catalytic micro-pyrolysis, coupled with sensitive detection techniques, may allow to follow the first intermediates in reactions of fatty acids transformations and the trends in the formation of hydrocarbons compatible with

liquid fuels.<sup>17</sup> This technique was used by Fonseca *et al.*<sup>2</sup> for pyrolysis of dilaurin, observing the formation of ketones as intermediates for hydrocarbons production.

This work aims to compare two different catalysts, Nb<sub>2</sub>O<sub>5</sub> and  $\gamma$ -Al<sub>2</sub>O<sub>3</sub> in the production of a long chain ketone, heptacosanone (K27), intermediate in the production of hydrocarbons, during micro-pyrolysis of tetradecanoic acid (C14:0) as a model fatty acid. The  $\gamma$ -Al<sub>2</sub>O<sub>3</sub> is a catalyst that show good activity in ketonization and hydrocarbon formation, and Nb<sub>2</sub>O<sub>5</sub> is an oxide showing reported redox properties, but scarcely used pure according to our knowledge, in catalytic fast pyrolysis<sup>18,19</sup> or in ketonization reactions.<sup>7,20,21</sup>

## Experimental

### Catalyst preparation

The catalyst Nb<sub>2</sub>O<sub>5</sub> was obtained by calcination at 700 °C, in air, for 2 h, of niobic acid (HY-340) supplied by Companhia Brasileira de Metalurgia e Mineração (CBMM), from Araxás, Minas Gerais, Brazil; its purity determined by X-ray fluorescence was greater than 99.8%. The Al<sub>2</sub>O<sub>3</sub> (A1) catalyst, supplied by Alcoa Alumínio S/A, São Paulo, Brazil, is a  $\gamma$ -alumina containing 0.013% of silica and 0.48% of sodium oxide, pore volume 0.9 cm<sup>3</sup> g<sup>-1</sup>.

### Preparation of samples used in pyrolysis experiments

For pyrolysis reactions, tetradecanoic acid-C14:0 (Sigma-Aldrich, St. Louis, USA), purity of 99%, was used after its “impregnation” on the surface of both catalysts. The powdered catalysts were hand mixed with C14:0 in a ratio of 10:1 (catalyst mass:tetradecanoic acid mass) by stirring and friction with glass rod, first at laboratory temperature and then at 95 °C, temperature higher than the melting point of the acid, in order to promote the diffusion of the liquid fatty molecules on the total surface of the solid materials. The prepared samples are referred to as C14:0/catalyst, “catalyst” being alumina or niobia.

### Characterization of catalysts

#### X-ray diffraction (XRD)

The X-ray diffraction experiment was performed using an XRD-6100 diffractometer from (Shimadzu, Kyoto, Japan), using Cu K $\alpha$  radiation. The diffractograms were collected in a 2 $\theta$  range of 10-80°, at a scanning rate of 1° min<sup>-1</sup>. Voltage and current used were 40 kV and 30 mA, respectively. The crystalline phases identification was performed using the X'Pert High Score software.

#### Brunauer-Emmett-Teller (BET) surface area

N<sub>2</sub> adsorption was performed at -196 °C using a BET equipment from Quantachrome Instruments (Ostfildern, Germany), model NOVA 2200. Prior to measurement, the samples were out gassed *in situ* under vacuum up to 350 °C (10 °C min<sup>-1</sup>, plus 30 min at 350 °C, after steps of 15 min at 100 and 200 °C). The surface area determinations were made with the option multi spread points, using five points of P/P<sub>0</sub> N<sub>2</sub> from 0.05 to 0.3. The manufacturer guarantees specific surface area analyzes as low as 0.01 m<sup>2</sup> g<sup>-1</sup>, due to the high accuracy of the pressure transducers, reaching 2 × 10<sup>-5</sup> of resolution for the relative pressures P/P<sub>0</sub> of N<sub>2</sub>.

#### Temperature programmed desorption of ammonia-TPD-NH<sub>3</sub>

TPD analysis were performed using a Micromeritics (Georgia, USA) Chemsorb, model 2720. The samples (100 mg) were preheated at 300 °C for 1 h under pure helium flow (30 mL min<sup>-1</sup>) and cooled to 28 °C. Adsorption of ammonia was performed using a 10% ammonia-helium mixture (30 mL min<sup>-1</sup>, 1 h). The weakly adsorbed ammonia was removed at 150 °C under pure helium flow (30 mL min<sup>-1</sup>) for 1 h. The thermo-desorption of the remaining adsorbed ammonia was performed between room temperature and 800 °C (10 °C min<sup>-1</sup>), also under helium flow. The amount of desorbed ammonia was monitored using a thermal conductivity detector. The calibration method was done using the standard mixture 10% ammonia-helium.

#### Fourier transform infrared spectroscopy (FTIR)

Pure tetradecanoic acid and both catalysts, pure or after adsorption of C14:0, were mixed with KBr and pelletized. The resulting disks were analyzed by FTIR at room temperature (23 °C), under ambient atmosphere using a Bomen (New South Wales, Australia) spectrophotometer model MB 102.

#### Pyrolysis

Pyrolysis reactions were done using a Frontier Laboratories LTD (Fukushima, Japan) Multi-Shot Pyrolyzer Model EGA/PY-3030D connected online with a gas chromatograph coupled to mass spectrometer Agilent (Santa Clara, California, USA) GC-MS 5799A. A Frontier Laboratories UA5-30M-0.25F GC column was used (30 m length, 0.25 mm diameter, 5% diphenyl stationary phase and 95% dimethylpolysiloxane, 0.25  $\mu$ m film thickness), subjected to an initial temperature of 40 °C for 2 min, followed by a heating ramp at a rate of 20 °C min<sup>-1</sup> up to 320 °C, temperature maintained for 10 more minutes.

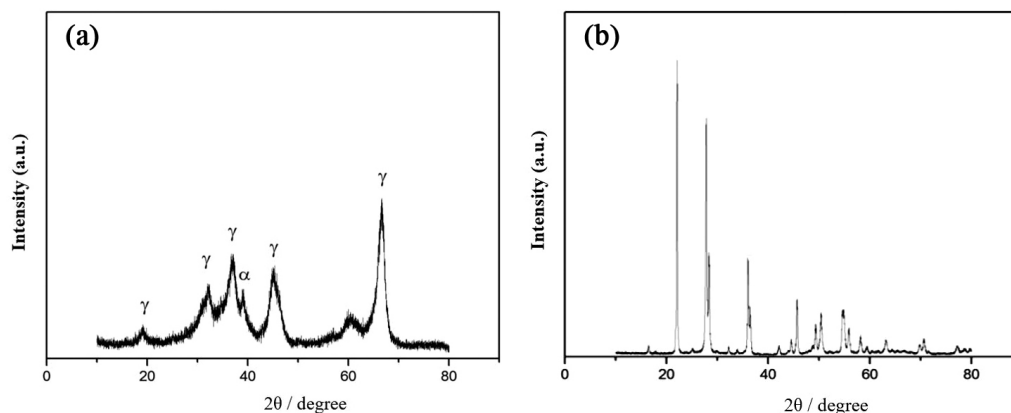


**Figure 2.** (a)  $\text{Al}_2\text{O}_3$  X-ray diffractogram; (b)  $\text{Nb}_2\text{O}_5$  X-ray diffractogram.

The MS ion source and the interface pyrolyzer/injector temperatures were both fixed at 320 °C. Values of  $m/z$  were set in the range of 40 to 400, in scan mode.

A mass of 2 mg of the C14:0/catalyst sample or 0.2 mg of pure tetradecanoic acid was inserted into a deactivated stainless-steel sample holder (Eco-cup LF PY1-EC80F, Frontier LAB) and covered with a thin layer of quartz wool prior to the pyrolysis experiments. The sample holder was then placed in the equipment under helium flow for purging, and the micro-pyrolyzer furnace was preheated to the desired pyrolysis temperature (450 or 600 °C). After stabilization, the sample holder was dropped instantly into the hot zone where it remained for 15 s at the chosen temperature. An aliquot of the gas phase was automatically inserted into the GC-MS equipment. Both the transfer lines from the inlet and outlet (to the GC-MS) are kept at an intermediate temperature, 320 °C.

For the analysis of the products, the chromatographic peaks with area lower than 0.5% of the total area were neglected. The peaks were identified using the NIST Database,<sup>22</sup> and only those products with identification probability greater than 80% were considered. The estimated compositions of ketones and hydrocarbons after pyrolysis were calculated dividing the peak areas of these specific products by the total area of the non-neglected peaks, including both the non-identified products and the remaining reactant, tetradecanoic acid. The standard deviation of the data was calculated and then implemented to the bar graphs using the STDEV function of the software Excel.<sup>23</sup>

## Results and Discussion

The X-ray diagram shown in Figure 2a confirms that the alumina used is essentially in the  $\gamma$ -phase (PDF10-0425) with major diffraction lines at  $2\theta = 46.2$  and  $67.2^\circ$ . The niobium oxide XRD diagram, Figure 2b, presented well defined diffraction lines at  $2\theta = 16.5, 22.1, 25.1, 27.8,$

$28.3, 31.2, 36.1, 42.1, 44.5, 45.6, 49.3, 50.4, 54.7, 55.8, 58.1, 59.4, 63.1^\circ$ , suggesting a material with orthorhombic crystalline structure (PDF 01-071-0336).

The BET measurements (Table 1) showed that the niobium oxide had a low specific surface area ( $4.4 \text{ m}^2 \text{ g}^{-1}$ ), coherent with values found in the literature<sup>24</sup> while the alumina presented a specific surface area of  $69.4 \text{ m}^2 \text{ g}^{-1}$ , in agreement with the data supplied by the manufacturer ( $71 \text{ m}^2 \text{ g}^{-1}$ ).

**Table 1.** Specific Brunauer-Emmett-Teller (BET) ( $S_{\text{BET}}$ ) surface area of the catalysts

Sample	$S_{\text{BET}} / (\text{m}^2 \text{ g}^{-1})$
$\gamma\text{-Al}_2\text{O}_3$	69.4
$\text{Nb}_2\text{O}_5$	4.4

Paulis *et al.*<sup>25</sup> showed that the increase of the calcination temperature produced a decrease in the surface area of niobium oxides: the samples calcined at 673, 773, 973 and 1173 K were found to possess surface areas of 144, 79, 16 and  $4 \text{ m}^2 \text{ g}^{-1}$ , respectively. The choice of the method for preparing or conditioning one catalyst is also due to the choice of the reaction conditions. In the present work, as the pyrolysis was carried out at 450 and 600 °C, the calcination of niobia was carried out at 700 °C, to improve its stability. The obtained specific surface area is lower than that obtained by these authors in similar calcination conditions, fact ascribed to different preparation methods and precursors.

Analyzes of TPD- $\text{NH}_3$  revealed that  $\text{Nb}_2\text{O}_5$  shows negligible acidity, and that  $\gamma\text{-Al}_2\text{O}_3$  had acid sites with different strengths (three ranges, showed in Table 2). The total amount of ammonia adsorbed on the alumina was  $2.4 \text{ mmol g}^{-1}$ , number equivalent to the acid sites concentration, being the majority of them strong acid sites.

Figure 3 presents the thermodesorption profiles of adsorbed ammonia on the catalysts  $\gamma\text{-Al}_2\text{O}_3$  and  $\text{Nb}_2\text{O}_5$  from

**Table 2.** Quantification and strength classification of the acidic sites of  $\gamma$ -Al<sub>2</sub>O<sub>3</sub>

Maximum desorption temperature / °C	Moles of NH <sub>3</sub>	Number of acid sites / (mmol g <sup>-1</sup> )	Strength of acid sites
159	$5.9 \times 10^{-5}$	$5.5 \times 10^{-1}$	weak
236	$6.5 \times 10^{-5}$	$6.1 \times 10^{-1}$	medium
400-600	$13.0 \times 10^{-5}$	$12.2 \times 10^{-1}$	strong
Total		$23.8 \times 10^{-1}$	

ambient temperature to 800 °C, showing the acid sites of  $\gamma$ -Al<sub>2</sub>O<sub>3</sub> with different strengths, as quantified in Table 2, and also revealing that Nb<sub>2</sub>O<sub>5</sub> shows negligible acidity. The  $\gamma$ -Al<sub>2</sub>O<sub>3</sub> ammonia desorption profile shows clearly the presence and predominance of strong acid sites, with temperature maxima above 400 °C.

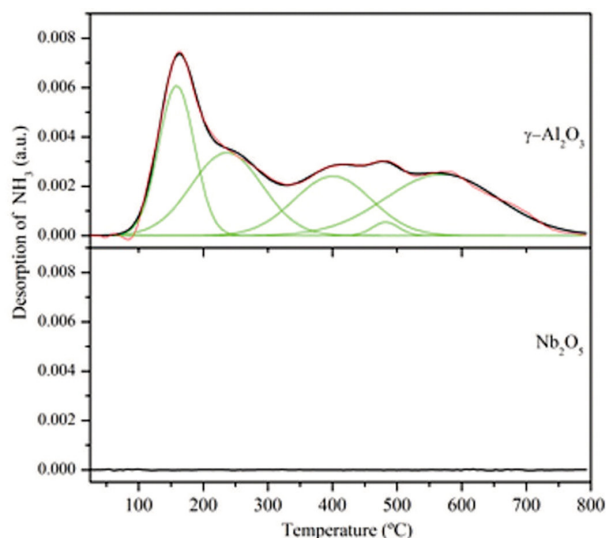
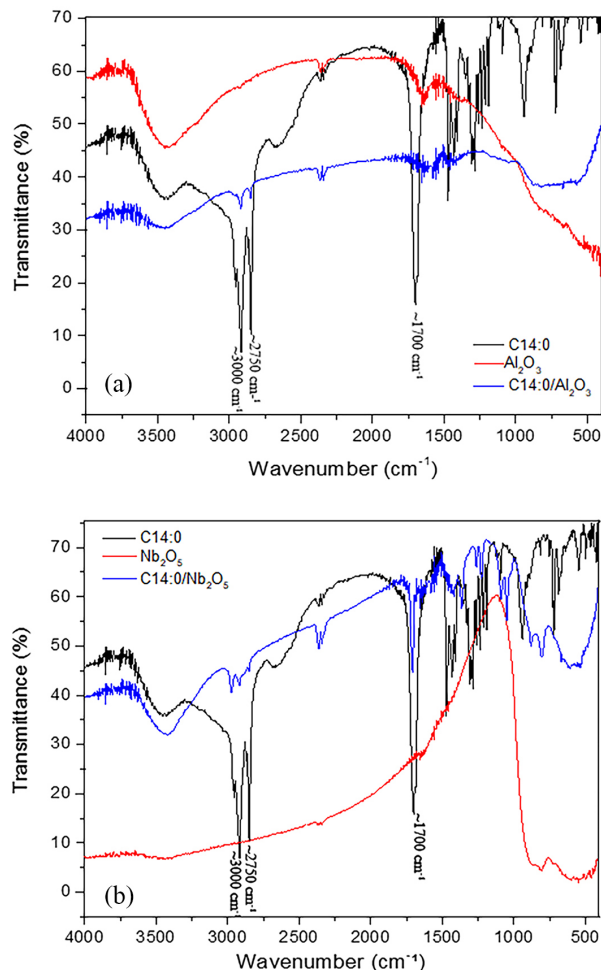
**Figure 3.** Thermodesorption profiles of adsorbed ammonia on the catalysts  $\gamma$ -Al<sub>2</sub>O<sub>3</sub> and Nb<sub>2</sub>O<sub>5</sub> from ambient temperature to 800 °C.

Figure 4 shows the FTIR spectra of the tetradecanoic acid, either pure or after the mixture with the  $\gamma$ -Al<sub>2</sub>O<sub>3</sub> (Figure 4a) and Nb<sub>2</sub>O<sub>5</sub> (Figure 4b) catalysts, as well as the spectra of the pure catalysts. The intense bands between 2750 and 3000 cm<sup>-1</sup> seen in tetradecanoic acid spectrum are due to the stretching of C–H in CH<sub>2</sub> and CH<sub>3</sub> groups. These bands still appear after contact with both alumina and niobia catalysts, less intense due to the dilution effect (about 10 wt.% of tetradecanoic acid/catalyst). The more intense band of tetradecanoic acid at about 1700 cm<sup>-1</sup>, is ascribed to C=O stretching vibration. This band practically disappears after mixing tetradecanoic acid with alumina (Figure 4a), suggesting that chemisorption occurred through the terminal COOH group. This result is in agreement with preceding work using palmitic acid and alumina as catalyst.<sup>21</sup>

**Figure 4.** FTIR (KBr) spectra: (a) pure  $\gamma$ -Al<sub>2</sub>O<sub>3</sub> (red line), pure tetradecanoic acid (black line), tetradecanoic acid after mixture with  $\gamma$ -Al<sub>2</sub>O<sub>3</sub> (blue line); (b) pure Nb<sub>2</sub>O<sub>5</sub> (red line), pure tetradecanoic acid (black line), tetradecanoic acid after mixture with Nb<sub>2</sub>O<sub>5</sub> (blue line).

This latter band is still present in the case of tetradecanoic acid mixed with niobia (Figure 4b), suggesting that, conversely to the alumina catalyst, a large amount of tetradecanoic acid is probably still present as free acid molecules after mixing with niobia, although a true quantification is not possible.

Figure 5 presents the amount of tetradecanoic acid remaining after pyrolysis, showing the positive effect of the temperature and of the presence of catalysts, the alumina promoting much higher C14:0 conversion (45% at 600 °C) than uncatalyzed pyrolysis and pyrolysis in presence of niobia.

The results showed also that at the lower temperature (450 °C), the presence of both catalysts clearly stimulated the formation of the ketone, the niobia catalyst being very selective for 14-heptacosanone, but with low conversion, less than 3%. The alumina catalyst exhibited the higher conversion to ketones at both temperatures, and a considerable fraction of these compounds was converted

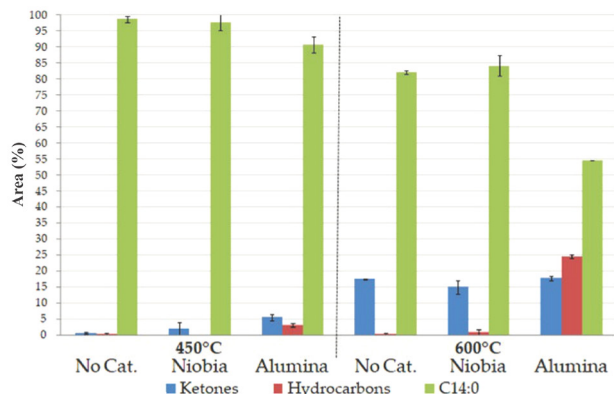


**Figure 5.** Percent of C14:0 non reacted, percent hydrocarbons and ketones formed at pyrolysis temperatures of 450 and 600 °C, without catalyst and with niobia and alumina catalysts.

to hydrocarbons.

Figure 5 shows further that even in absence of catalyst, the transformation of tetradecanoic acid to 14-heptacosanone is possible. More specifically, at 600 °C, the ketone amount observed after thermal pyrolysis is comparable to the one observed in presence of both alumina and niobia catalysts. The main difference is that, in absence of catalyst, the further transformation of the ketone to hydrocarbons did not occur to a significant extent. In the pyrolysis at 600 °C with the niobia catalyst, ketones yield was about 15%, and some hydrocarbons were seen (about 2%), while with the alumina catalyst, 56% of the tetradecanoic acid was converted, hydrocarbons being the main products of the reaction (about 24%), followed by ketones (about 18%).

The conversion of tetradecanoic acid in the temperature range used, by comparison with other studies using this model molecule and other pyrolysis set up showed important differences, suggesting that the equipment geometry and the experimental details can lead to different reacting environment. In preceding studies, using a pyrolysis temperature of 650 °C, the uncatalyzed pyrolysis of C14:0 practically did not allow to observe conversion: vapors of C14:0 were directly conducted to the analytical system, without suffering transformation.<sup>17,26</sup>

Conversely, Zafar *et al.*,<sup>27</sup> when pyrolyzing C14:0 at 650 °C obtained a quite large conversion, the main product being 1-dodecene. These authors also observed various small chain carboxylic acids and other lower carbon chain 1-alkenes. A small amount of *n*-tridecane was also identified in this latter work, but no ketone has been detected during pyrolysis by opposition to the results of the present study. Although there is a 50 °C difference in pyrolysis temperature between the study of Zafar *et al.*,<sup>27</sup> and the maximum temperature used here, the preceding results suggest that the longer transfer line

from the pyrolysis section to the analytical one increases the possibility of condensation of heavy pyrolysis products. Both Zafar *et al.*<sup>27</sup> and Santos *et al.*<sup>21</sup> used similar equipment with a long transfer line kept at 320 °C, and the 14-heptacosanone has a normal boiling point of 453.7 °C. The present study was performed without transfer line, in a set up with very short transfer space, limiting the possibility of condensation. This fact could explain the discrepancies related to ketones detection. Even though, different performances in the same setup are meaningful and can be discussed.

Anand *et al.*<sup>28</sup> observed that MgO and ZrO<sub>2</sub> catalysts promoted the formation of long chain ketones by fast pyrolysis of lipid-rich microalga, *Schizochytrium limacinum*, in the temperature range of 350 to 650 °C. With MgO, at 400 °C nearly 85% of the carbonyl group was constituted by 16-hentriacontanone (30%), 14-heptacosanone (22%) and 2-nonadecanone (9%). The mechanism of formation of the first two ketones can be attributed to selfketonization reaction of palmitic (C16) and myristic acids (C14) inherently present in the algae, while other ketones are formed by the ketonization of acetic acid formed during pyrolysis with palmitic and myristic acids.

Corma *et al.*<sup>29</sup> also studied the ketonic decarboxylation of carboxylic acids. Basic magnesium oxide was used as catalyst to carry out this reaction in a fixed-bed continuous reactor. With lauric acid (C12), complete conversion was achieved in less than one hour of contact time at 400 °C. At 95% conversion, the desired ketone (C<sub>11</sub>H<sub>23</sub>COC<sub>11</sub>H<sub>23</sub>, laurone) was obtained with excellent selectivity (97%).

The results presented in Figure 5 allow us to conclude that the conversion of tetradecanoic acid to hydrocarbons, with formation of the intermediate 14-heptacosanone, is favored using the highest pyrolysis temperature (600 °C) and alumina catalyst. At this temperature, the yield of remaining 14-heptacosanone was 18% and the yield of hydrocarbons 24%. Higher temperatures could promote the transformation of ketones to hydrocarbons, with probably an increase in light and isomerized products.

Figures 6a and 6b present two pyrograms of tetradecanoic acid transformation, obtained respectively in the presence of alumina and niobia, at the same temperature, i.e., 600 °C. In Figure 6a, significant amounts of 1-dodecene (C12) on the light fraction of chemical compounds, and of 14-heptacosanone (K27) on the heavy compounds side of the pyrogram are observed. In Figure 6b, however, 14-heptacosanone is the main product observed. In both cases, unconverted reactant tetradecanoic acid (C14:0) is also present.

The 14-heptacosanone is formed by direct association of two tetradecanoic acid molecules through their acid

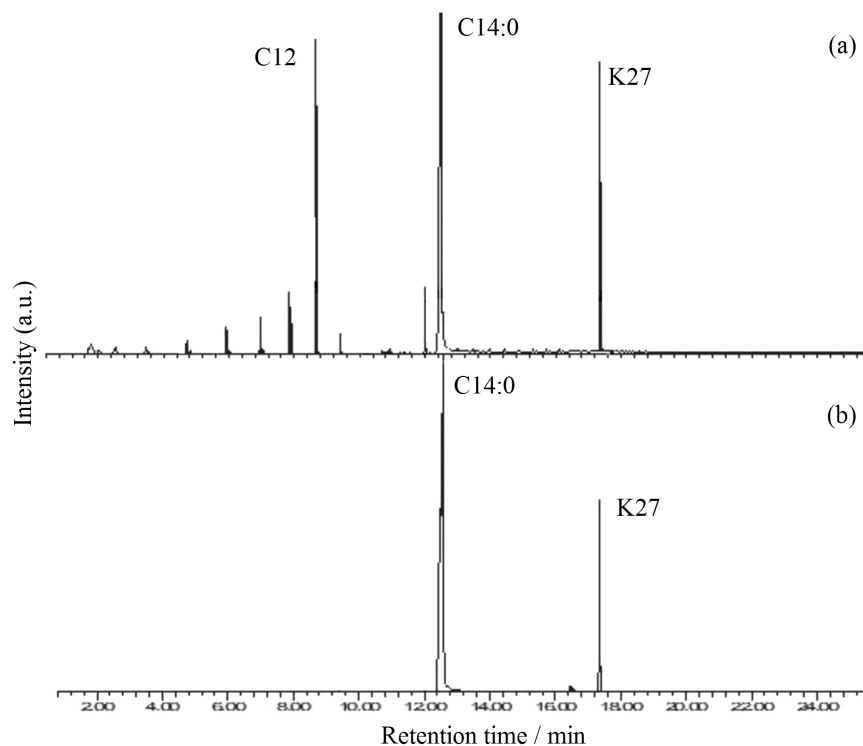


**Figure 6.** Total pyrogram of tetradecanoic acid (C14:0) adsorbed on alumina (a) and niobia (b), at 600 °C, showing some of the main products observed. (C12) 1-dodecene, (K27) 14-heptacosanone.

functional group with elimination of  $\text{CO}_2$  and  $\text{H}_2\text{O}$ . A significant quantity of other hydrocarbons is also observed when performing pyrolysis with alumina, essentially 1-dodecene (C12) and hydrocarbons with carbon chain length lower than C12. Although both pyrograms are quite different, the identified products and their distribution are, at least in part, in line with the mechanism of fatty compounds cracking suggested in the literature<sup>25,27</sup> in which ketones are considered as intermediates products during thermal deoxygenation of fatty acids.

The extended pyrogram windows shown in Figures 7a and 7b detailed some typical aspects of these results for pyrolysis with the alumina catalyst. On the light fraction of chemical compounds (Figure 7a), the formation of C9 to C14 hydrocarbons is observed, the main hydrocarbons being 1-alkenes and *n*-alkanes. In these pyrolysis conditions, an increase in the ratio *n*-alkane/1-alkene is observed in Figure 7a when going from C9 to C11, but this ratio decreases to *quasi* 0 for the C12 products in which 1-dodecene is the main hydrocarbon formed.

On the heavy compounds side (Figure 7b), three main compounds were identified: 2-pentadecanone, untransformed tetradecanoic acid (C14:0) and 14-heptacosanone (K27), as well as many other compounds such as different ketones, mainly unsymmetrical, and hydrocarbons having carbon chain length greater than C14. In these latter fractions, despite the fact that the probability

of identification is not always as high as 80%, the nature of identified ketones and hydrocarbons seems guaranteed, as the homologous character of these products is quite clear.

Generally, the cracking of saturated fatty acids or saturated fatty acid sodium salts leads to the formation of homologue hydrocarbon families containing principally unsaturated and saturated linear molecules, the products with major amount having lost one carbon atom in their carbon chain by comparison with the chain length of the starting fatty acid.<sup>30,31</sup> Such result was not obtained in the present conditions, as the main hydrocarbon detected possesses a C12 carbon chain (1-dodecene, Figure 7a), i.e., has lost 2 carbon atoms by comparison with the chain length of the original reactant, tetradecanoic acid, fact also observed by Zafar *et al.*<sup>27</sup> This observation suggests that this compound was not obtained by direct acid decarbonylation or decarboxylation mechanisms. A split of the 14-heptacosanone associated to a  $\gamma$ -hydrogen transfer mechanism, with the production of an enol and a 1-alkene probably explains the formation of 1-dodecene as major hydrocarbon product as well as 2-pentadecanone, as residual part of the initial 14-heptacosanone. The formation of an enol producing a methyl ketone (here 2-pentadecanone) has been suggested in the literature.<sup>4,8,20,32</sup> In the present work, a deeper cracking of the alkyl chains of 14-heptacosanone initially formed may also occur, justifying, although in very limited amount, the presence of long chain ketones

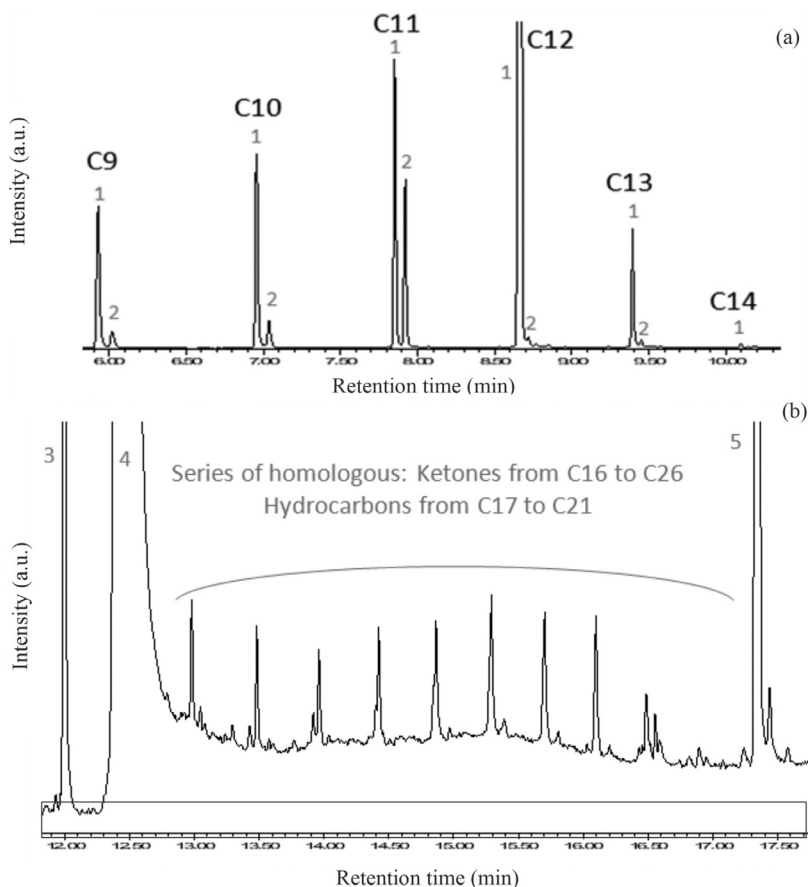


**Figure 7.** Pyrograms fragments of C14:0 pyrolysis at 600 °C in presence of alumina between (a) retention times 6.0 and 10.0 min, showing specific hydrocarbons ( $C_n$ ): (1) 1-alkenes and (2)  $n$ -alkanes; and (b) between 12.0 to 17.5 min, showing specific products: (3) 2-pentadecanone; (4) tetradecanoic acid (C14:0); (5) 14-heptacosanone (K27).

and hydrocarbons as well as small chain length alkenes and alkanes, also observed before.<sup>4,27,33</sup> Hydrocarbons with carbon chain equal or longer than that of tetradecanoic acid, from C14 to C21 were observed in the present work, for example, 10-heneicosene. These products can result from deoxygenation and cracking of unsymmetrical and symmetrical ketones (essentially 14-heptacosanone), through reduction/dehydration mechanism, as shown in Figure 1. Billaud *et al.*,<sup>4</sup> Oliver-Tomas *et al.*,<sup>6</sup> as well as Leung *et al.*<sup>20</sup> and Corma *et al.*<sup>29</sup> using carboxylic acids, performed pyrolysis reactions leading to the formation of ketones and hydrocarbons, both with chain length larger than that of the starting carboxylic acid, similar to the results presented in Figure 7b.

The conversion of carboxylic acids and the resulting products distribution may have complex relationship with catalyst properties. In their study of carboxylic acid ketonization in presence of metal oxides, Pestman *et al.*<sup>7</sup> concluded that the higher the M–O bond strength, the greater the conversion to ketones. Kumar *et al.*<sup>9</sup> stated that neighbor basic and acid sites are necessary to promote the formation of symmetrical ketones.

In the present study,  $Nb_2O_5$  shows very low BET area and negligible acidity, whereas  $\gamma-Al_2O_3$  presented a surface area comparatively high ( $69.4 \text{ m}^2 \text{ g}^{-1}$ ) and a rather significant acidity. A high surface area may promote the interaction of primary pyrolysis products with surface sites, leading to secondary pyrolysis reactions, forming both low and high molecular weight hydrocarbons, fact also observed with alumina as catalyst, during the cracking of carboxylic and fatty acids.<sup>4,21</sup> On the contrary, the low surface area of niobia and the absence of acidity may favor the presence of the intermediate product, here 14-heptacosanone, limiting its transformation. Lu *et al.*<sup>34</sup> concluded that ketonization reaction can be increased by using oxides having good redox properties. Niobium oxide can present some redox properties in reducing atmosphere, allowing transformation of  $Nb^{5+}$  to  $Nb^{4+}$ , at temperatures above 400–500 °C, favoring partially deoxygenated products.<sup>35</sup>

Two other mechanisms, occurring in parallel to ketonization, are able to promote the formation of hydrocarbons from fatty acids: the first one is decarbonylation producing CO,  $H_2O$  and terminal alkenes and the second one decarboxylation producing  $n$ -alkanes

and CO<sub>2</sub>,<sup>20,36</sup> both leading to the formation of molecules with one less carbon atom in their chain, compared to the original fatty acid. Although these mechanisms are well documented, the formation of small chain hydrocarbons starting from saturated fatty acid may imply a further cracking mechanism, essentially at the higher temperature used here, 600 °C. The cracking of the fatty molecule could occur not only close to the functional group COOH, but also along the carbon chain. Such a mechanism generates small carboxylic acids and short chain hydrocarbons and was demonstrated in pyrolysis of triglycerides and saturated fatty acids.<sup>26,27,37,38</sup> Small chain carboxylic acids in the reaction medium can participate to the formation of unsymmetrical ketones (Figure 7b) as well as small chain hydrocarbons, principally 1-alkenes, also observed here (Figure 7a).

## Conclusions

Ketones and hydrocarbons production through catalytic pyrolysis of tetradecanoic acid depends heavily on the temperature and catalyst nature. At 450 °C, Nb<sub>2</sub>O<sub>5</sub> catalyst was very selective for 14-heptacosanone formation, but with low conversion, less than 3%. The γ-Al<sub>2</sub>O<sub>3</sub> catalyst promoted better deoxygenation and cracking, leading to different families of products such as 1-alkenes and *n*-alkanes.

Within the conditions used, the conversion of tetradecanoic acid to hydrocarbons, with formation of the intermediate 14-heptacosanone, is favored using the highest pyrolysis temperature (600 °C) and alumina catalyst. At this temperature, the yield of 14-heptacosanone was 18% and the yield of hydrocarbons 24%.

Fast pyrolysis is therefore an important technique to verify the nature of intermediate reaction compounds such as 1-dodecene and 2-pentadecanone produced from 14-heptacosanone cracking. The present experimental work confirmed also the possibility to obtain hydrocarbons having a chain length larger than the chain length of the original fatty acid reagent, due to a ketonization route followed by decarbonylation.

The conversion of tetradecanoic acid at 600 °C allowed the formation of C3-C12 hydrocarbons using transition γ-alumina as catalyst. These products can be used as drop in fractions in fuels such as liquified petroleum gas, gasoline, kerosene and probably diesel, when using fatty molecules with greater carbon chains.

## Acknowledgments

This paper was prepared with the financial support of

the Bahia State Research Support Foundation (FAPESB), Higher Education Personnel Improvement Coordination (CAPES) and the National Council for Scientific and Technological Development (CNPq), Brazil. Furthermore, the authors are grateful to the following laboratories of the Federal University of Bahia (UFBA): Coordination Chemistry Research Group (GPQC) for the assistance in FTIR analysis, Laboratory of Catalysis and Materials (LABCAT) for the TPD-NH<sub>3</sub> analysis, and the Catalysis and Environment Laboratory (CATAM) for the XRD and BET analysis.

## References

1. Jimenez, S. E.; Crocker, M.; *J. Chem. Technol. Biotechnol.* **2012**, *87*, 1041.
2. Fonseca, N.; Pereira, A.; Frety, R.; Sales, E. A.; *Catalysts* **2019**, *9*, 993.
3. Renz, M.; *Eur. J. Org. Chem.* **2005**, *2005*, 979.
4. Billaud, F.; Minh Tran, A. K.; Lozano, P.; Pioch, D.; *J. Anal. Appl. Pyrolysis* **2001**, *58-49*, 605.
5. Vavon, G.; Apchie, A.; *Bull. Soc. Chim.* **1928**, *43*, 667.
6. Oliver-Tomas, B.; Renz, M.; Corma, A.; *Chem. - Eur. J.* **2017**, *23*, 12900.
7. Pestman, R.; Koster, R. M.; Pieterse, J. A. Z.; Ponc, V.; *J. Catal.* **1997**, *168*, 255.
8. Pham, T. N.; Sooknoi, T.; Crossley, S. P.; Resasco, D. E.; *ACS Catalysis* **2013**, *3*, 2456.
9. Kumar, R.; Enjamuri, N.; Shah, S.; Al Fatesh, A. S.; Juan, J. B. S.; Chowdhury, B.; *Catal. Today* **2018**, *302*, 16.
10. Murzin, D. Y.; Bernas, A.; Warnå, J.; Myllyoja, J.; Salmi, T.; *React. Kinet., Mech. Catal.* **2018**, *126*, 601.
11. Qiao, Y.; Wang, B.; Zong, P.; Tian, Y.; Xu, F.; Li, W.; Li, F.; Tian, Y.; *Energy Convers. Manage.* **2019**, *199*, 1119664.
12. Hasanudin, H.; Rachmat, A.; Said, M.; Wijaya, K.; *Period. Polytech., Chem. Eng.* **2020**, *64*, 238.
13. Yenumala, S. R.; Maity, S. K.; Shee, D.; *React. Kinet., Mech. Catal.* **2017**, *120*, 109.
14. Boekaerts, B.; Sels, B. F.; *Appl. Catal., B* **2021**, *283*, 119607.
15. Lee, K.; Kim, M. Y.; Choi, M.; *ACS Sustainable Chem. Eng.* **2018**, *6*, 13035.
16. Huo, X.; Huq, N. A.; Stunkel, J.; Cleveland, N. S.; Starace, A. K.; Settle, A. E.; York, A. M.; Nelson, R. S.; Brandner, D. G.; Fouts, L.; St. John, P. C.; Christensen, E. D.; Luecke, J.; Mack, J. H.; McEnally, C. S.; Cherry, P. A.; Pfefferle, L. D.; Strathmann, T. J.; Salvachúa, D.; Kim, S.; McCormick, R. L.; Beckham, G. T.; Vardon, D. R.; *Green Chem.* **2019**, *21*, 5813.
17. Fréty, R.; Pacheco, J.; Santos, M.; Padilha, J.; Azevedo, A.; Brandão, S.; Pontes, L.; *J. Anal. Appl. Pyrolysis* **2014**, *109*, 56.
18. Simão, B. L.; Santana Jr., J. A.; Chagas, B. M. E.; Cardoso, C. R.; Ataíde, C. H.; *Algal Res.* **2018**, *32*, 221.

19. Brandão, R. F.; Quirino, R. L.; Mello, V. M.; Tavares, A. P.; Peres, A. C.; Guinhos, F.; Rubim, J. C.; Suarez, P. A. Z.; *J. Braz. Chem. Soc.* **2009**, *20*, 954.
20. Leung, A.; Boocock, D. G. B.; Konar, S. K.; *Energy Fuels* **1995**, *9*, 913.
21. Santos, M. R.; Arias, S.; Padilha, J. F.; Carneiro, M. C. N.; Sales, E. A.; Pacheco, J. G. A.; Fréty, R.; *Catal. Today* **2020**, *344*, 234.
22. *National Institute of Standards and Technology*; version NIST 08, Gaithersburg, USA, 2020.
23. *Microsoft Excel*, version Excel 2007, Microsoft Corporation, Redmond, Washington, USA, 2020.
24. Raba, A. M.; Ruiz, J. B.; Joya, M. R.; *Mater. Res.* **2016**, *19*, 1381.
25. Paulis, M.; Martin, M.; Soria, D.; D'iaz, A.; Odrizola, J.; Montes, B.; *Appl. Catal., A* **1999**, *180*, 411.
26. Santos, M. R.; Sales, R. F.; Silva, A. O. S.; Teixeira, C. M.; Pacheco, J. G. A.; Fréty, R.; *J. Therm. Anal. Calorim.* **2015**, *119*, 1875.
27. Zafar, R.; Watson, J. S.; Weiss, D. J.; Sephton, M. A.; *J. Anal. Appl. Pyrolysis* **2017**, *123*, 184.
28. Anand, V.; Gautam, R.; Vinu, R.; *Fuel* **2017**, *205*, 1.
29. Corma, A.; Renz, M.; Schaverien, C.; *ChemSusChem* **2008**, *1*, 739.
30. Maher, K. D.; Bressler, D. C.; *Bioresour. Technol.* **2007**, *98*, 2351.
31. Lappi, H.; Alén, R.; *J. Anal. Appl. Pyrolysis* **2011**, *91*, 154.
32. March, J.; *Advanced Organic Chemistry: Reactions, Mechanisms and Structures*, 6<sup>th</sup> ed.; Wiley: New Jersey, USA, 2007.
33. Asomaning, J.; Mussone, P.; Bressler, C. D.; *J. Anal. Appl. Pyrolysis* **2014**, *105*, 1.
34. Lu, F.; Jiang, B.; Wang, J.; Huang, Z.; Liao, Z.; Yang, Y.; *Mol. Catal.* **2018**, *444*, 22.
35. Wachs, I. E.; Jehng, J. M.; Deo, G.; Hu, H.; Arora, N.; *Catal. Today* **1996**, *28*, 199.
36. Vonghia, E.; Boocock, D. G. B.; Konar, S. K.; Leung, A.; *Energy Fuels* **1995**, *9*, 1090.
37. Kubátová, A.; Luo, Y.; Štřáková J.; Sadrameli, S. M.; Aulich, T.; Kozliak, E.; Seames, W.; *Fuel* **2011**, *90*, 2598.
38. Lima, D. G.; Soares, V. C. D.; Ribeiro, E. B.; Carvalho, D. A.; Cardoso, E. C. V.; Rassi, C. F.; Mundim, K. C.; Rubim, J. C.; Suarez, P. A. Z.; *J. Anal. Appl. Pyrolysis* **2004**, *71*, 987.

Submitted: November 24, 2021

Published online: March 28, 2022

